Planta (1990) 180:312–323

Planta

The occurrence of unusual laminated structures rich in β-1,4-glucans in plastids of *Phaseolus vulgaris* root-nodule cells infected by an ineffective C_4-dicarboxylic-acid mutant of *Rhizobium leguminosarum* bv. *phaseoli*

Pierre J. Lafontaine [1]*, Nicole Benhamou [2], and Hani Antoun [1]

[1] Département des Sols and [2] Département de Phytologie, Université Laval, Québec G1K 7P4, Canada

Abstract. Root nodules induced in *Phaseolus vulgaris* L. by the wild-type (WT) and a C_4-dicarboxylic-acid mutant strain of *Rhizobium leguminosarum* biovar. *phaseoli* were compared on the basis of ultrastructure and cytochemistry of cellulose subunits. The mutant bacteroids failed to colonize infected host cells in a normal manner, and presented a premature degenerative appearance. Starch granules, rough endoplasmic reticulum and mitochondria were found to accumulate in the ineffective nodules. The most striking difference between effective and ineffective nodules was the presence of unusual spherical, laminated structures in plastids of mutant-infected host cells only. Cytochemical observations showed that these structures contain β-1,4-glucans. The presence of β-1,4-glucans within such structures may be caused by the activity of a cellulase which is produced by either the bacteroids or the host cell and is locally hydrolyzing the host cell-wall, thus releasing cellulose subunits into the cytoplasm. Another possibility is de-novo synthesis of β-1,4-glucans in the host cell.

Key words: β-1,4-Glucan – Nitrogen fixation – *Phaseolus* (root nodules) – *Rhizobium* (mutant) – Root nodules produced by mutant *Rhizobium*

* To whom correspondence should be addressed; *present address:* Institut botanique de l'Université de Montréal, 4101 rue Sherbrooke Est, Montréal, Qué., Canada H1X 2B2

Abbreviations in text: PBS = phosphate-buffered saline; PEG = polyethylene glycol; PHB = poly-β-hydroxybutyrate; RER = rough endoplasmic reticulum; TTC = 2,3,5-triphenyl tetrazolium chloride; WT = wild-type

Abbreviations in figures: B, bacteroid; *C*, cortex; *Cy*, cytoplasm; *CC*, central core; *HCW*, host cell-wall; *IC*, infected cell; *IS*, intercellular space; *LS*, laminated structure; *N*, nucleus; *P*, peroxisome; *PHB*, poly-β-hydroxybutyrate; *Pl*, plastid; *PlM*, plastid matrix; *PM*, peribacteroid membrane; *RER*, rough endoplasmic reticulum; *S*, starch grain; *UC*, uninfected cell; *Va*, vacuole; *VB*, vascular bundle

Introduction

The symbiotic association of *Rhizobium* with legumes results in the formation of specialized structures, the root nodules, where fixation of atmospheric dinitrogen occurs. Root nodule formation proceeds through a series of sequential events including deformation and invasion of root hairs, development of infection threads, initiation of cell divisions, and elaboration of nodule tissue with release and differentiation of bacteria into bacteroids (for a recent review see e.g. Long and Cooper 1988).

Symbiotic effectiveness may be severely altered by unfavorable environmental conditions or by genetic variations within both partners. In recent years, there has been a great deal of progress in our understanding of the various mechanisms leading to ineffective association between *Rhizobium* and legumes. Considerable attention has been paid to the defects that could be responsible for the formation of ineffective nodules, including the inability of bacteria to penetrate root hairs (Van den Bosch et al. 1985) or to be released from infection threads (Bergersen 1957; Pankhurst 1974), premature senescence of bacteroids (MacKenzie and Jordan 1974), and the lack of peribacteroid membranes (Newcomb et al. 1977; Selvaraj et al. 1987). Interest has also been devoted to cell-surface polysaccharides in mutants of several *Rhizobium* species (e.g. Leigh and Lee 1988). Since polysaccharides exposed at the cell surface are known to be key determinants in recognition events (Dazzo and Truchet 1983) it is to be expected that any alteration in sugar composition at the surface of *Rhizobium* mutants may be responsible for the formation of less or even non-effective nodules (Leigh et al. 1987; Doherty et al. 1988; Long et al. 1988).

Formation of ineffective nodules may also be caused by *Rhizobium* mutant strains that are defective in the uptake or metabolism of C_4-dicarboxylic acids. Recent studies dealing with such *Rhizobium* mutants on several

legumes have shown that C_4-dicarboxylic acids were closely involved in the nitrogen-fixation process (Ronson et al. 1981; Finan et al. 1983; Arwas et al. 1985; Lafrenière et al. 1987; Watson et al. 1988). These data support the hypothesis of Ronson et al. (1981) according to which C_4-dicarboxylic acids are the main source of energy and reducing power for bacteroids. Premature senescence of nodules induced by such mutants was reported in clover (Ronson et al. 1981) and alfalfa (Watson et al. 1988) although such senescence was not observed in the case of pea root nodules (Finan et al. 1983). Other observations of pea root nodules conducted at the electron-microscope level showed a pronounced breakdown of peribacteroid membranes (Arwas et al. 1985). By contrast, little is known about the ultrastructure of effective and naturally ineffective wild-type strains of *Rhizobium* in *Phaseolus vulgaris* (Nogueira et al. 1979; Baird and Webster 1982).

In an attempt to address this question, we have compared, in the present study, the ultrastructure of *P. vulgaris* root nodules induced by the effective wild-type strain P_{121} of *Rhizobium leguminosarum* bv. *phaseoli* and its ineffective C_4-dicarboxylic-acid mutant $P_{121}S_{21}$. These observations were extended to the study of the distribution of cellulosic β-1,4-glucans in both nodule types by gold cytochemistry (Benhamou et al. 1987; Benhamou 1989). The detection of laminated structures rich in cellulosic β-1,4-glucans in plastids of mutant-infected cells is a new finding that raises the question of both the origin and nature of these unusual structures.

Material and methods

Bacterial strains. P_{121} is a wild-type (WT) strain isolated from a Quebec soil and classified as a very effective strain on French bean cv. Goldie (Lalande et al. 1986) and $P_{121}S_{21}$ is a C_4-dicarboxylic-acid ineffective mutant of this strain, induced by N-methyl-N′-nitro-N-nitrosoguanidine (NTG). $P_{121}S_{21}$ is a putative C_4-dicarboxylic-acid transport mutant having a functional tricarboxylic-acid cycle. This mutant has been previously characterized (Lafontaine et al. 1989a).

Mutagenesis. A log-phase culture of strain P_{121} was treated with 200 µg/ml NTG for 30 min at 25° C. The treated cells were washed twice with 3 mM phosphate-buffered saline (PBS), pH 6.8, suspended in BM_1-mannitol broth defined medium (Lafrenière et al. 1987) and incubated for 24 h at 28° C on a rotary shaker (160 rpm), to allow segregation and expression of mutations. For enrichment, the cells were washed twice in PBS and resuspended in BM_2 defined medium (Lafrenière et al. 1987) supplemented with 10 mM succinate and 500 µg/ml carbenicillin. After incubation at 28° C for 24 h on a rotary shaker, the enrichment cycle was repeated. Enriched cultures were washed, and plated for single colonies on BM_2-succinate medium modified by using 0.6 $g \cdot l^{-1}$ proteose peptone as a nitrogen source and by adding filter-sterilized 2,3,5-triphenyl tetrazolium chloride (TTC) to a final concentration of 25 $\mu g \cdot l^{-1}$. On this medium, WT colonies displayed satisfactory growth and reduced TTC (pink colonies), while mutants showed poor growth and did not reduce TTC (white colonies).

Plant material. Seeds of *Phaseolus vulgaris* L. cv. Goldie were surface-sterilized in 6% aqueous NaOCl for 10 min, followed by six rinses in sterile water. The seeds were germinated on sterile cotton for 3–4 d and then planted in sterilized vermiculite. After emergence, seedlings were carefully removed from the pots and inoculated by soaking the roots in a fresh liquid culture of strain P_{121} or strain $P_{121}S_{21}$ (10^8–10^9 cells $\cdot$ ml^{-1}). Inoculated seedlings were then immediately transferred into a sterilized hydroponic growth system, containing an N-free modified Hoagland's solution (Lafontaine et al. 1989b). Plants were grown at 23 ± 2° C with a 16-h daily light period under cool-white fluorescent lamps. Fifteen days after inoculation, root nodules were harvested. They corresponded to the stage where maximum acetylene-reduction activity was recorded for the effective strain P_{121} (Lafontaine et al. 1989b).

Tissue processing. Root nodules were excised with a razor blade, sliced, and immersed in a freshly prepared solution of 2.5% (v/v) glutaraldehyde in 0.1 M sodium-cacodylate buffer, pH 7.2, for 2 h under vacuum. The samples were then rinsed with the same buffer, dehydrated in a graded series of ethanol, and embedded in Epon 812. Thick sections (0.5 µm) were collected on glass slides and stained by the basic fuchsin-methylene blue method according to Huber et al. (1968). Ultrathin sections (0.1 µm) collected on formvar-coated nickel grids were contrasted with aqueous uranyl acetate and lead citrate, and examined in a Siemens (FRG) Elmiskope electron microscope or a JEOL (Japan) 1200 EX electron microscope.

Purification and properties of the exoglucanase used for the localization of cellulosic β-(1,4)-linkages. The exoglucanase, a β-(1,4)-glucan cellobiohydrolase (EC 3.2.1.91) was purified in a five-step procedure from a cellulase produced by the cellulolytic fungus *Trichoderma harzianum* Rifai. The purification procedure was performed according to Berghem and Pettersson (1973) and consisted in group fractionation by molecular-sieve chromatography, double ion-exchange chromatography on diethylaminoethyl (DEAE)-Sephadex 50, gel filtration on a polyacrylamide P-150 column and affinity chromatography on Concanavalin A-Sepharose column and on SP-Sephadex cation exchanger. Enzyme purity was verified by analytical polyacrylamide gel electrophoresis and by isoelectric focusing in flat-bed polyacrylamide gels. The exo-β-1,4-glucanase activity was tested against Avicel (a commercial crystalline cellulose powder) and carboxymethylcellulose according to Berghem et al. (1975). It was estimated to be 20 U/mg, one unit being the amount of enzyme needed to liberate reducing sugars equivalent to 100 µg of glucose under the assay conditions. The exoglucanase was able to degrade about 80% of microcrystalline cellulose within a few hours. The data from the isoelectric focusing indicated an optimal pH of 5.0–5.6.

Cytochemical labeling. Colloidal gold with particles averaging 15 nm in diameter was prepared according to Frens (1973). The exoglucanase was complexed to gold at pH 9.0 according to the procedure described in Benhamou et al. (1987). Red pellets, collected after ultracentrifugation at 13000 rpm for 60 min at 4° C, were recovered in 0.5 ml of PBS, pH 6.0, containing 0.02% polyethylene glycol 20000 (PEG 20000).

Sections were first floated on a drop of PBS-PEG, pH 6.0, for 5 min, then transferred on a drop of the exoglucanase-gold complex diluted 1:2 in PBS-PEG, pH 6.0, for 30 min at room temperature in a humid chamber (Benhamou et al. 1987). They were then rinsed with PBS and distilled water, and contrasted with uranyl acetate and lead citrate.

Specificity of labeling was assessed by means of the following control tests: 1) incubation with the exoglucanase-gold complex to which had been added β-1,4-glucans from barley (1 mg/ml); 2) incubation with the uncomplexed enzyme followed by treatment with the corresponding gold-complexed exoglucanase; 3) incubation with a nonenzyme-gold complex such as albumin-gold complex; 4) incubation with the stabilized gold suspension alone.

Chemicals and supplies. Avicel was purchased from American Viscose Co., Marcus Hook, Penn., USA. All reagents used for enzyme purification were obtained from Pharmacia, Baie D'Urfe, Qué., Canada. Tetrachloroauric acid was purchased from BDH Chemicals, Montréal, Que., and PEG 20000 from Fisher Scientific, Montréal. Reagents used for tissue processing were obtained from JBEM Co. Pointe-Claire, Qué. Products used for gold labeling and NTG, TTC and carbenicillin were purchased from Sigma Chemical Co., St. Louis, Mo., USA. Proteose peptone was obtained from Difco Laboratories, Detroit, Mich., USA. Seeds of *Phaseolus vulgaris* cv. Goldie were purchased from R. Rogers & Brothers Seed Co., Idaho Falls, Idaho, USA and cool-white fluorescent lamps from General Electric, Montréal.

Results

Nodule morphology. Nodules induced by wild-type *R. leguminosarum* bv. *phaseoli* (P_{121}) were visible on seedlings 7 d after inoculation. When fully developed (14 d after inoculation) they were spherical, displayed a pink color, and were grouped in clusters along the roots.

The mutant strain ($P_{121}S_{21}$) was also able to induce the formation of nodules. However, these nodules, which started to appear not before 9 d after inoculation, were morphologically different from those induced by the WT inoculum. In addition to being slightly smaller in size, they displayed a white to greenish color and were scattered throughout the roots instead of being clustered.

Histological observations. At the light-microscope level, examination of 0.5-µm longitudinal sections of nodules formed by the WT strain P_{121} showed that nodules were composed of an outer cortical zone containing vascular bundles, and an inner central area consisting of both infected and uninfected cells (Fig. 1). Densely stained infected cells were large and round, and appeared heavily packed with bacteroids whereas; uninfected cells were quite small and rectangular with a single central vacuole and peripherally located nuclei and amyloplasts (Fig. 1).

Observations of longitudinally sectioned mutant-induced nodules showed a cytological arrangement similar to that observed in nodules formed by the WT. Typical vascular bundles were present in the cortical area and the central zone was differentiated into large infected cells and small uninfected cells (Fig. 2). However, infected cells were found to stain lightly, thus implicating the occurrence of bacteroids dispersed in the host cytoplasm (Fig. 2). Uninfected cells interspersed among the infected ones contained several large amyloplasts that stained darkly and were peripherally located along the cell wall (Fig. 2). The substantial number of these amylo-

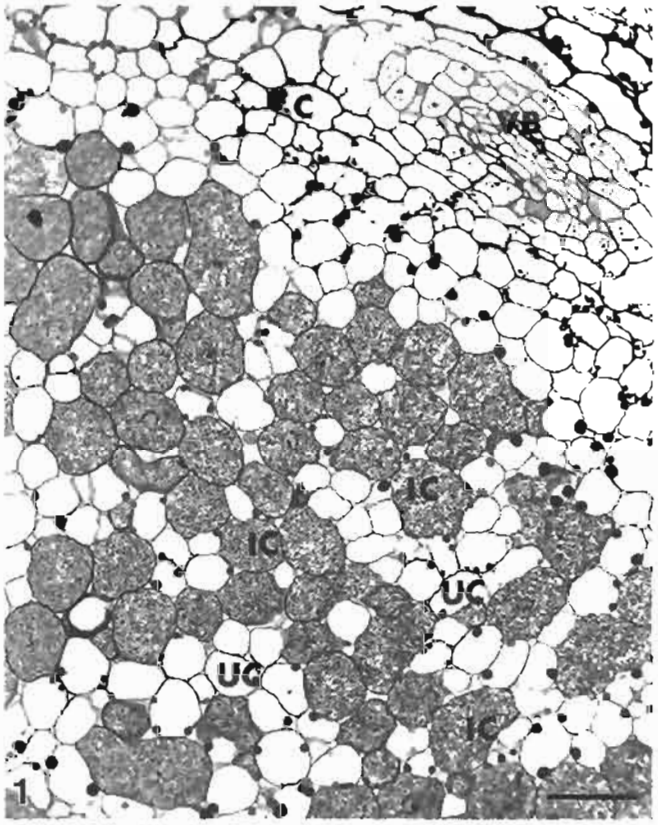

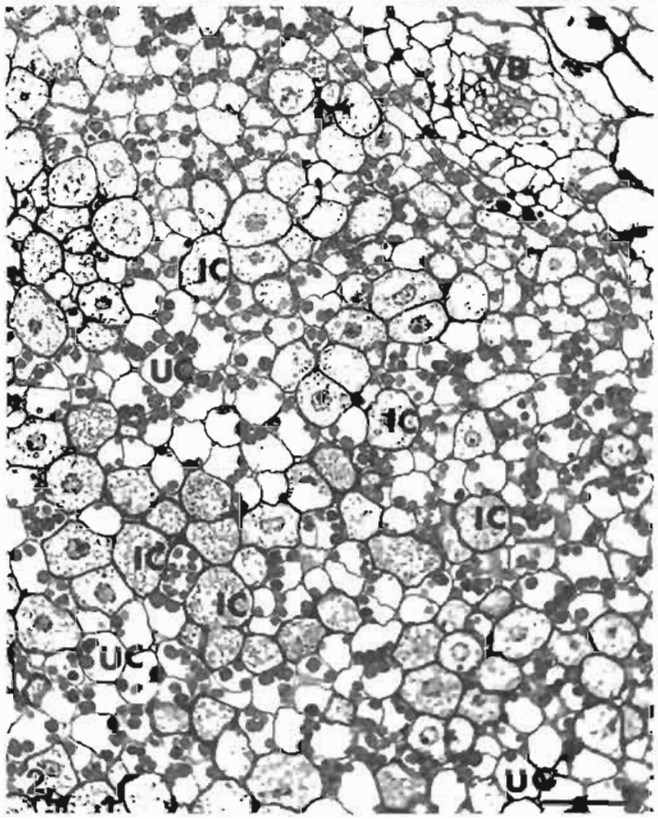

Figs. 1, 2. Light-microscope photographs of 15-d-old *P. vulgaris* root nodules infected by *Rhizobium leguminosarum* bv. *phaseoli*. ×1140; bar = 10 µm. **Fig. 1.** Nodule induced by the WT strain of *R. leguminosarum* bv. *phaseoli* (P_{121}). A vascular bundle is visible in the cortical area. In the central portion, large infected cells appear densely packed with bacteroids. Uninfected cells contain a central vacuole and peripherally located amyloplasts. **Fig. 2.** Nodule induced by the C_4-dicarboxylic-acid mutant strain of *R. leguminosarum* bv. *phaseoli* ($P_{121}S_{21}$). In the central portion, infected cells contain only few dispersed bacteroids. Uninfected cells are characterized by an accumulation of amyloplasts at the periphery

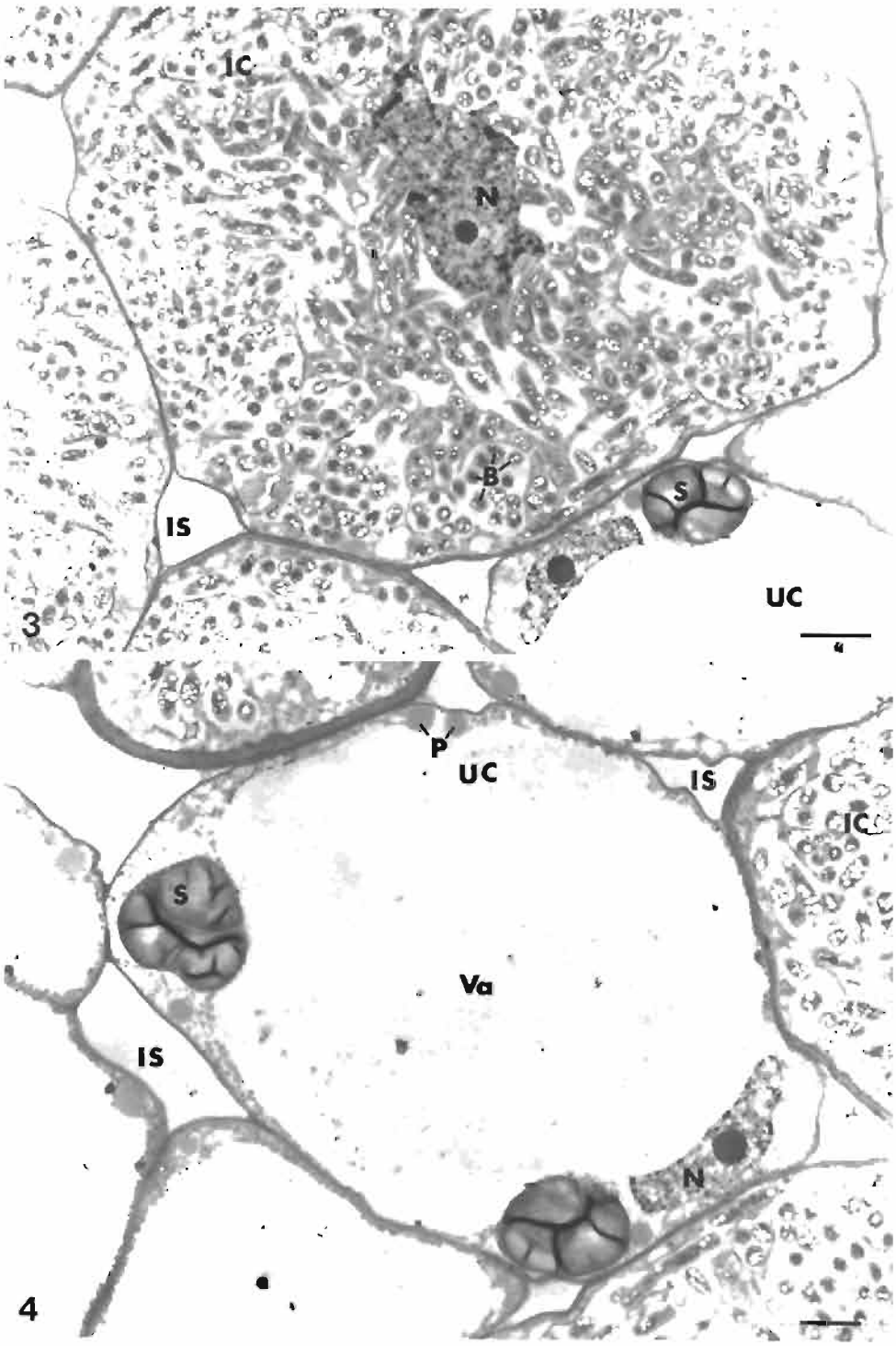

Figs. 3, 4. Transmission electron micrographs of the central portion of an effective root nodule in *P. vulgaris*. **Fig. 3.** Infected cells. Bacteroids occur in groups surrounded by wavy peribacteroid membranes. Vacuoles are absent and organelles are confined at the periphery. ×4500; bar = 2.5 μm. **Fig. 4.** Uninfected cells. A single, large vacuole is surrounded by remnants of cytoplasm. At the periphery of the cell, amyloplasts, nucleus and peroxisomes are visible. ×5000; bar = 2 μm

plasts in uninfected cells of mutant-induced nodules contrasted with the low amount of such structures in uninfected cells of effective nodules (Figs. 1, 2).

Ultrastructural observations. In the WT-induced nodules, examination at the electron-microscope level of 0.1-μm sections of nodules confirmed the occurrence of infected cells which appeared densely packed with bacteroids (Fig. 3). These cells were always devoid of vacuoles but generally exhibited a centrally located nucleus which could vary in size and shape. All other pre-existing organelles such as mitochondria and plastids were restricted to the periphery of the cells and were, very often, hardly discernible. The host cytoplasm was greatly reduced and appeared as fine, electron-opaque strands between peribacteroid membranes (Fig. 3). These membranes were irregularly shaped, depending apparently upon the number and distribution of enclosed bacter-

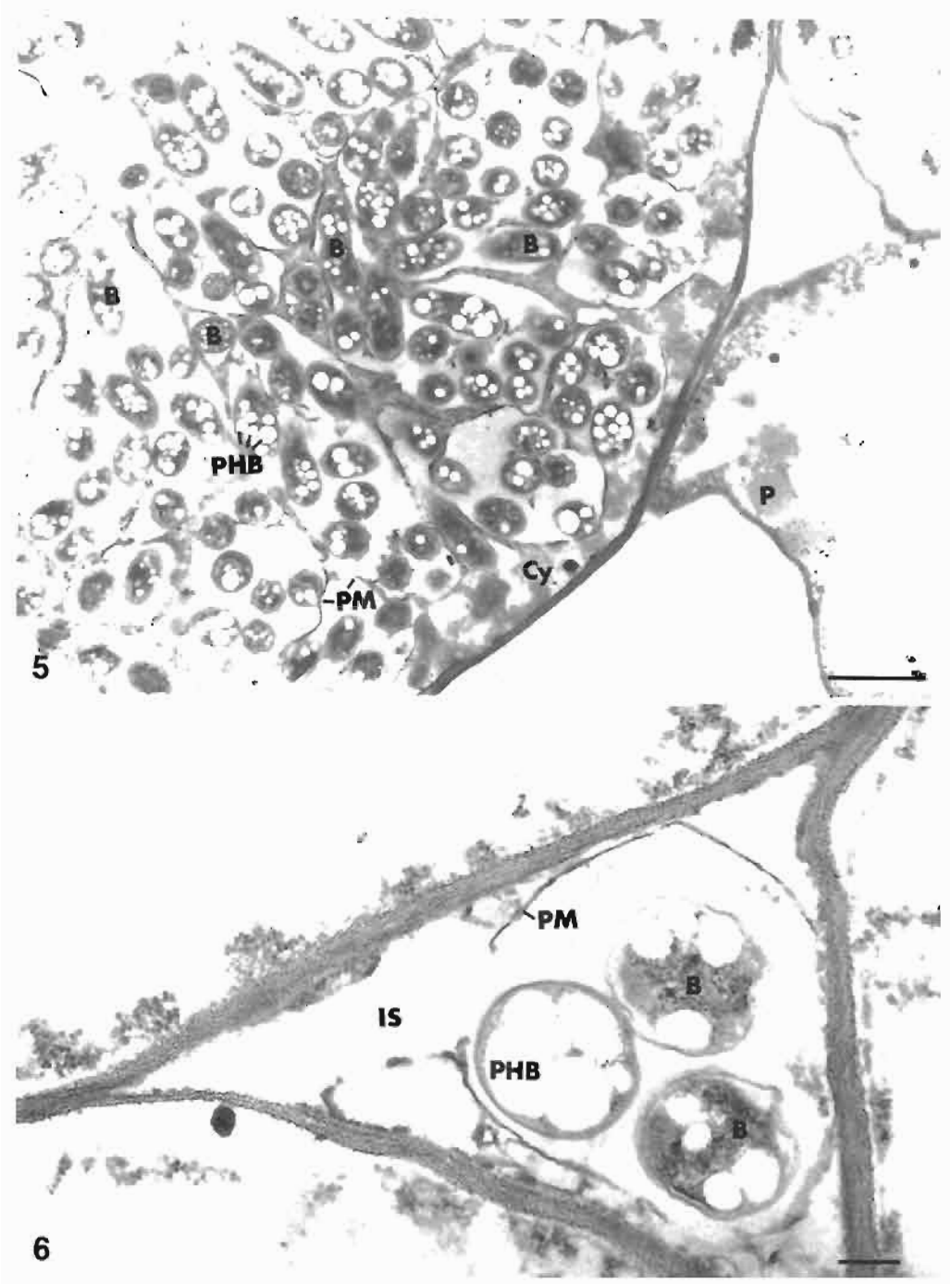

Figs. 5, 6. Transmission electron micrographs of the central portion of an effective root nodule in *P. vulgaris*. **Fig. 5.** High magnification; it is noticeable that bacteroids, grouped into peribacteroid membranes, contain substantial amounts of poly-β-hydroxybutyrate (*PHB*). ×11000; bar = 1.5 μm. **Fig. 6.** An intercellular space is colonized by three bacteroids which appear to be surrounded by an apparently disrupted peribacteroid membrane. ×48000; bar = 0.2 μm

oids. Uninfected cells typically had a single large vacuole, an elongated nucleus with an electron-dense nucleolus, and an average of two amyloplasts containing large starch granules (Fig. 4). In addition, electron-opaque microbodies resembling peroxisomes were found to occur mainly in cell areas adjacent to intercellular spaces.

At higher magnifications, it could be seen that bacteroids within infected cells occurred mainly in groups surrounded by wavy peribacteroid membranes (Fig. 5). Single bacteroids were seldom observed. Nearly all bacteroids contained electron-lucent deposits characteristic of poly-β-hydroxybutyrate (PHB). Infection threads that derived from an invagination of the host cell-wall were occasionally seen and were found to contain bacteria already enriched in PHB. Colonization of some intercellular spaces was observed (Fig. 6). Bacteroids enclosed in these spaces were surrounded by an envelope which was altered in some places and resembled a peribacteroid membrane (Fig. 6). This has already been reported in soybean root nodules (Werner and Mörschel 1978).

Ultrastructural observations of the central portion of mutant-induced nodules demonstrated pronounced morphological differences (Figs. 7–11). The most striking

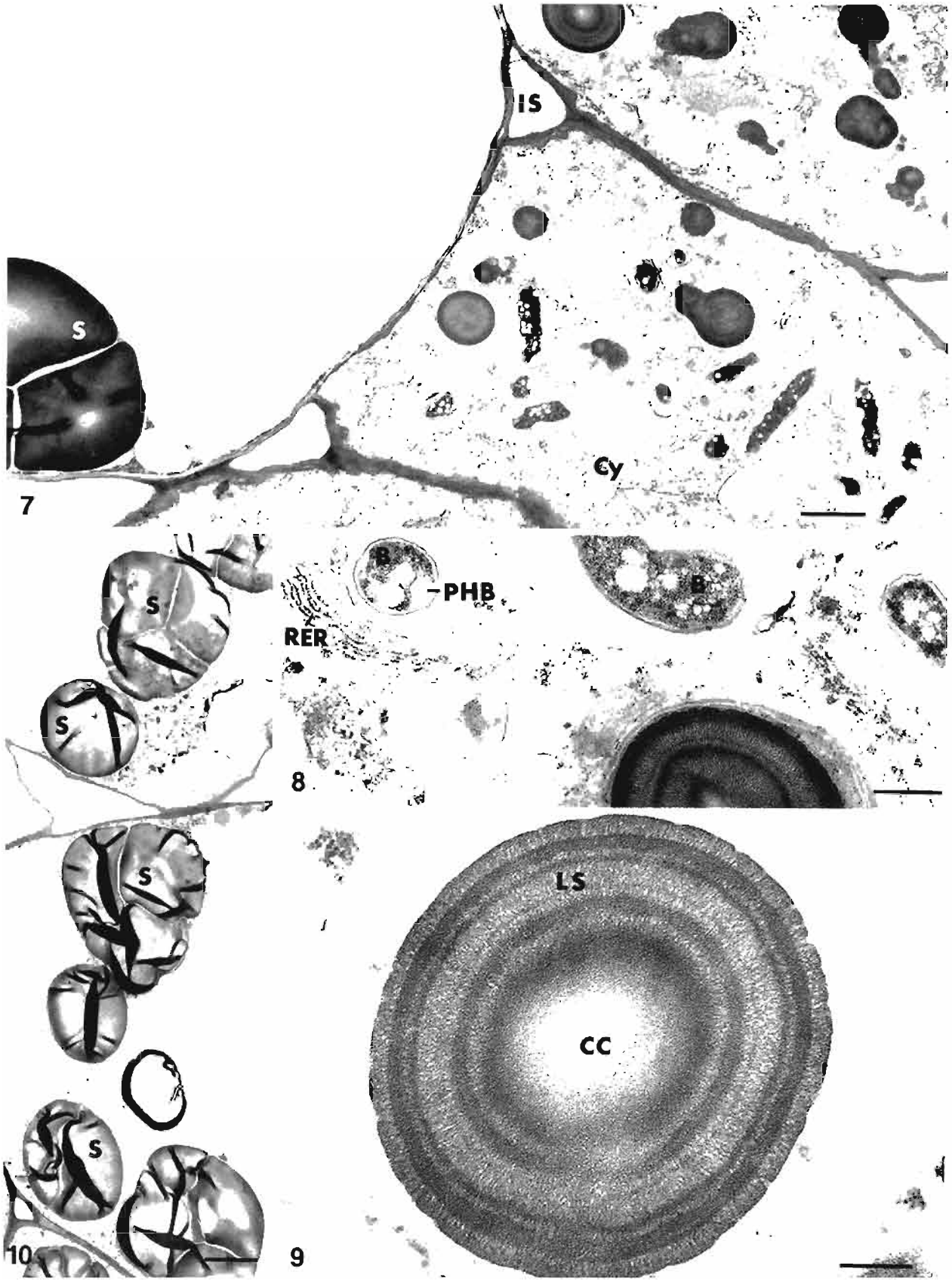

Figs. 7–10. Transmission electron micrographs of the central portion of an ineffective root nodule (induced by the C_4-dicarboxylic-acid mutant strain of *R. leguminosarum* bv. *phaseoli*) in *P. vulgaris*. Fig. 7. Infected cells contain fewer bacteroids dispersed in the cytoplasm. Spherical, laminated structures are present in the plastids. × 7200; bar = 1.5 μm. Fig. 8. At a higher magnification, stacks of rough endoplasmic reticulum (*RER*) are discernible. Bacteroids contain low amounts of PHB deposits. × 24000; bar = 0.5 μm. Fig. 9. Ultrastructural aspect of a laminated structure which is composed of an electron-lucent central core surrounded by successive laminations of different thickness and electron density. × 60000; bar = 0.2 μm. Fig. 10. Uninfected cells characterized by the presence of numerous amyloplasts containing large starch grains. × 5000; bar = 2 μm

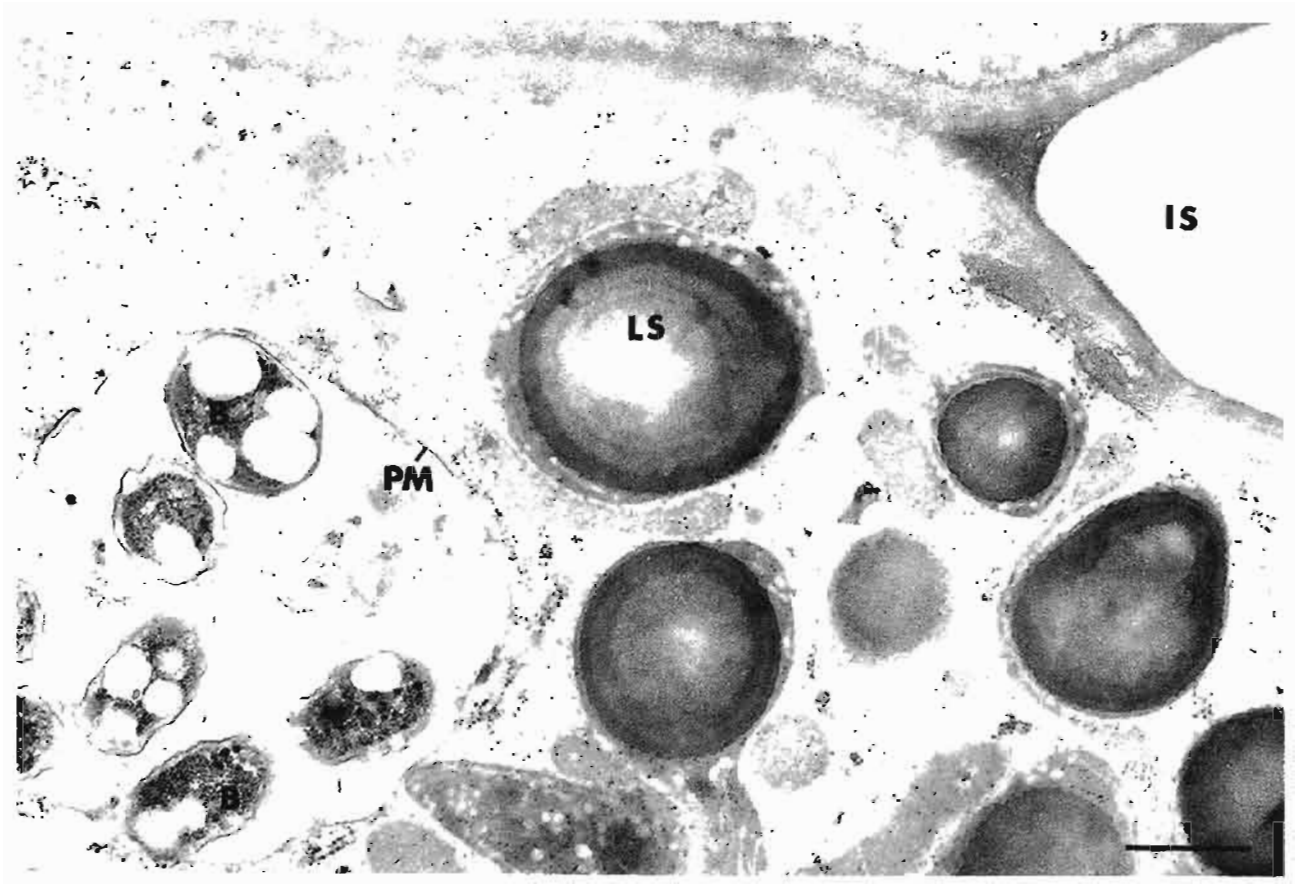

Fig. 11. Transmission electron micrographs of the central portion of an ineffective root nodule in *P. vulgaris*. Occasionally, bacteroids are grouped and surrounded by a peribacteroid membrane. Laminated structures contained in plastids are consistently present. ×36000; bar=0.45 μm

characteristic of this tissue was the occurrence of infected cells containing few bacteroids dispersed in an apparently preserved host cytoplasm where stacks of rough endoplasmic reticulum (RER) were discernible (Figs. 7, 8). This contrasted with effective nodules in which the cytoplasm was restricted to fine strands and RER segments were scattered. Cytoplasmic vacuolation occurred but was restricted to few small vacuoles scattered throughout the cytoplasm (Fig. 7). When visible, the nucleus had a tendancy to be lobed and was centrally located. Typical amyloplasts containing starch grains were not observed. Instead, spherical structures were consistently observed within plastids in infected cells (Figs. 7, 8). At high magnification, these unusual structures appeared to be composed of an electron-lucent, central core surrounded by successive laminae of different thickness and electron density (Fig. 9). Interestingly, many of the plastids containing such electron-opaque structures were surrounded, at least partially, by elongated organelles which closely reflected their contour (Fig. 11). From their structural appearance, such organelles recalled mitochondria. Although plastids containing spherical bodies were present in all infected cells, their number was found to vary greatly from one cell to another, ranging from 2 to 20 or more. Bacteroids were scattered throughout the host cytoplasm and most of them were surrounded singly by a peribacteroid membrane (Fig. 7). They showed a more or less degenerative appearance as judged by the partial cytoplasmic retraction frequently observed. In addition, they were found to contain fewer deposits of PHB than bacteroids observed in effective nodules. Infection threads were observed in the examined sections.

Uninfected cells of mutant-induced nodules were characterized by a large central vacuole surrounded by an accumulation of amyloplasts containing numerous, large starch grains (Fig. 10). The nucleus was usually small and confined to the periphery of the cell (Fig. 10). When compared with uninfected cells of WT induced nodules, the most striking difference was the considerable increase in starch granules. Small peroxisomes occurred in areas adjacent to intercellular spaces (Fig. 10).

Cytochemical observations. Incubation of ultrathin sections of either WT- or mutant-induced nodules resulted in an intense labeling of host cell-walls (Figs. 12, 14). Following treatment with the exoglucanase-gold complex, labeling was restricted to host cell-walls (Fig. 12) and infection threads (not shown) of nodules formed by the WT strain. In addition, plastids adjacent to the

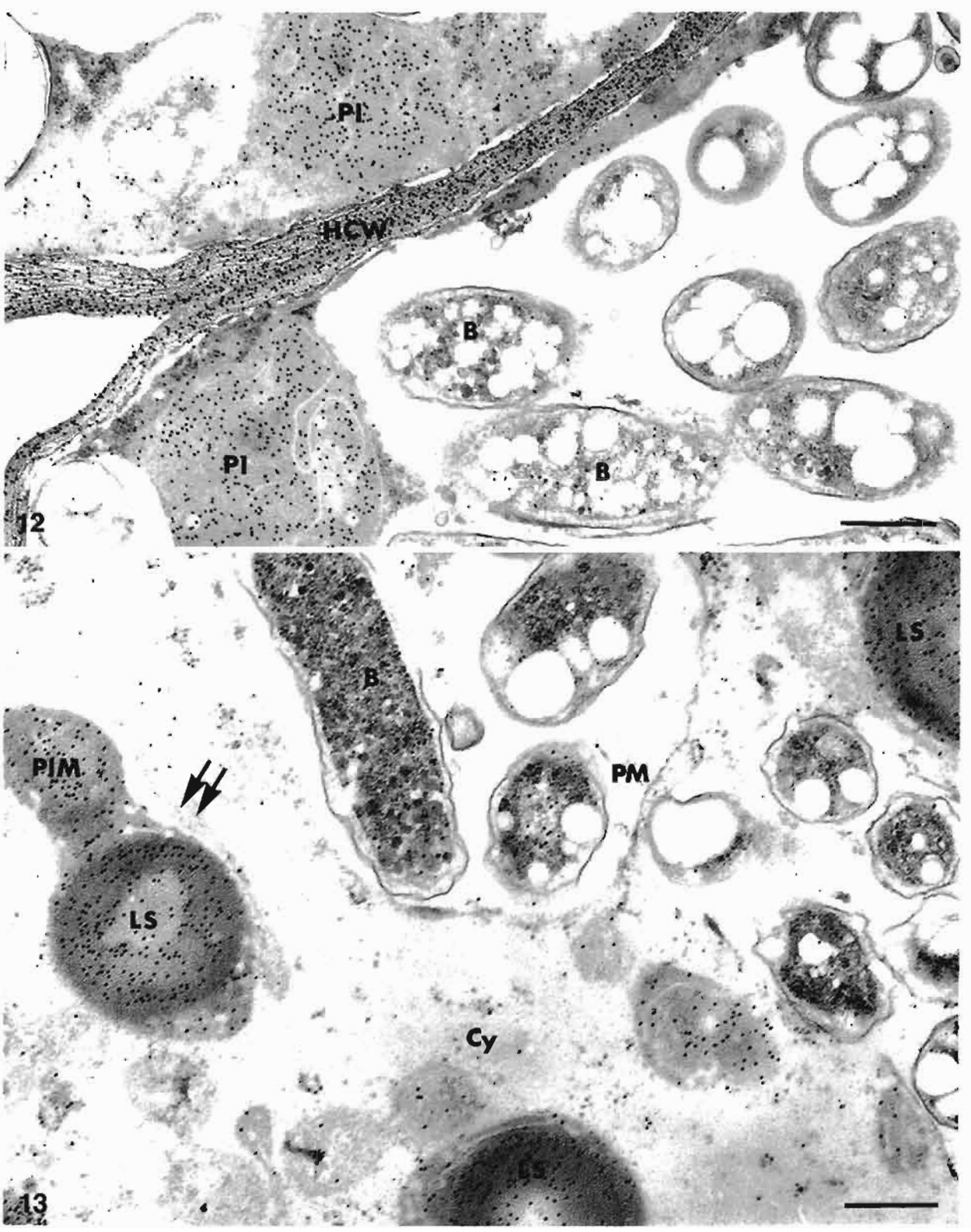

Figs. 12, 13. Transmission electron micrographs of the central portion of an effective and an ineffective root nodule of *P. vulgaris* respectively. Labeling of β-1,4-glucans with the exoglucanase-gold complex. × 36000; bar = 0.45 μm. Fig. 12. Host cell-walls and plastids are intensely and specifically labeled. Few scattered gold particles occur over bacteroids. Fig. 13. Gold particles are present over bacteroids. An intense labeling occurs over the spherical, laminated structures and plastids matrix

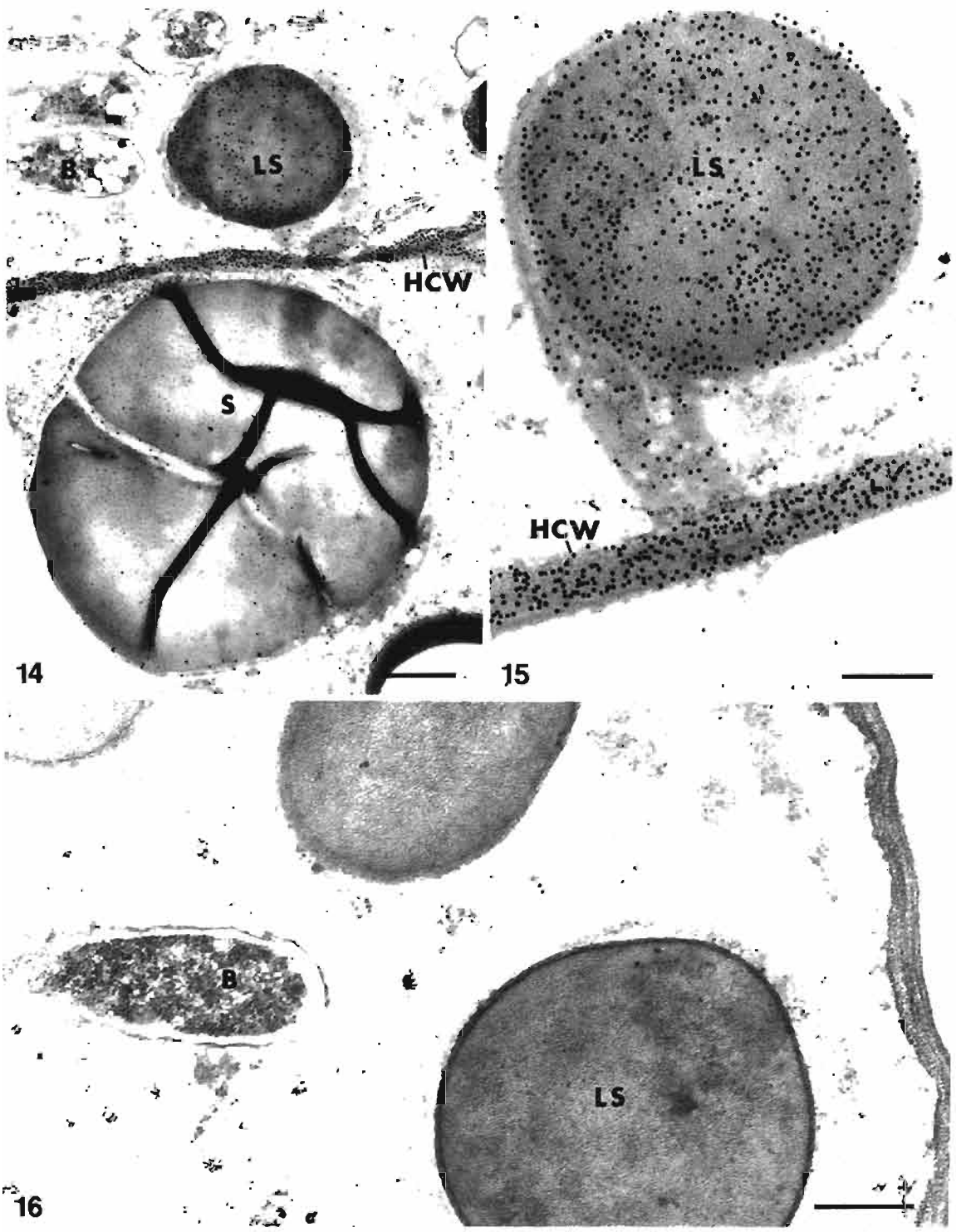

Figs. 14–16. Transmission electron micrographs of the central portion of an ineffective root nodule of *P. vulgaris*. Labeling of β-1,4-glucans with the exoglucanase-gold complex. **Fig. 14.** A laminated structure in an infected cell is heavily labeled whereas a starch grain in an adjacent uninfected cell is unlabeled. The host cell-wall is also specifically labeled. ×18000; bar = 0.7 μm. **Fig. 15.** A heavily labeled laminated structure in an infected cell and labeled plastid matrix. ×50000; bar = 0.3 μm. **Fig. 16.** Control test. Preadsorption of the exoglucanase-gold complex with an excess of β-1,4-glucans from barley prior to section treatment results in a near absence of labeling. ×36000; bar = 0.45 μm

cell wall were also densely labeled (Fig. 12). A similar labeling pattern was observed over infected cells of mutant-induced nodules (Fig. 13). Host cell-walls and infection-thread walls were specifically labeled whereas all other structures including host cytoplasm, RER, mitochondria and nuclei were nearly unlabeled (Figs. 13, 14). Few gold particles were associated with bacteroids and labeling was absent over peribacteroid membranes (Fig. 13). However, the most interesting finding was the intense labeling of the spherical, laminated structures occurring only in plastids of infected cells of mutant-induced nodules (Figs. 13, 15). Depending on the plane of sectioning, it appeared that gold particles were preferentially associated with the electron-opaque outer layers rather than with the electron-lucent central core (Fig. 13). The plastid matrix was also labeled by the gold-complex probe (Figs. 13, 15). The elongated organelles resembling mitochondria and closely surrounding plastids containing such layered structures were not substantially labeled (Fig. 13). Some plastids containing layered structures were in apparent connection with the adjacent host cell-wall (Fig. 15). However, this could be an optical effect caused by the plane of sectioning and – or the section thickness. Large starch grains, located at the periphery of uninfected cells, were devoid of labeling (Fig. 14). This absence of gold particles contrasted strongly with the strong and specific labeling of the spherical, laminated structures in neighbouring infected cells.

All control tests described in *Materials and methods*, including preadsorption of the gold complexed with β-1,4-glucans from barley prior to incubation of sections (Fig. 16), resulted in a near absence of labeling over host cell-walls and the spherical laminated structures.

Discussion

Although a number of studies have dealt with the ultrastructure of root nodules induced by C_4-dicarboxylic-acid mutants of some *Rhizobium* species (Ronson et al. 1981; Finan et al. 1983; Arwas et al. 1985; Watson et al. 1988) there seems to have been no report concerning the particular feature of nodules induced by the C_4-dicarboxylic-acid mutant $P_{121}S_{21}$ in *Phaseolus vulgaris*.

The most striking variations between the WT and mutant nodules were associated with the number of bacteroids and with specific organelles, namely endoplasmic reticulum, mitochondria and plastids. Infected cells of ineffective nodules were weakly colonized as judged by the low number of bacteroids, and these displayed a more or less degenerative appearance. Most of them were singly enclosed in peribacteroid membranes, thus indicating failure to divide after release from infection threads. In mutant-infected cells, the most typical features were the accumulation of RER, the occurrence of large number of mitochondria and vacuoles, and the presence of numerous multilayered, spherical structures.

In previous papers dealing with fix$^-$ nodules induced by C_4-dicarboxylic-acid mutants of other *Rhizobium* species, infected cells were reported to be filled with bacteroids that displayed a normal morphological appearance and were enclosed in peribacteroid membranes (Ronson et al. 1981; Finan et al. 1983; Arwas et al. 1985; Watson et al. 1988). In most cases, signs of premature nodule senescence were noted. Surprisingly, these particular features were not observed in the case of the mutant-induced nodules in *P. vulgaris* since bacteroids failed to colonize intensely infected cells and showed partial to complete disintegration, leading sometimes to the occurrence of empty peribacteroid envelopes. Such a degenerative process was recently described by Werner et al. (1984) in soybean root nodules induced by nod$^+$ fix$^-$ mutants of *Bradyrhizobium japonicum*.

Our observations demonstrated a considerable accumulation of RER and mitochondria in infected cells of ineffective *P. vulgaris* nodules. These results are in agreement with those reported by MacKenzie and Jordan (1974) and Baird and Webster (1982) on other types of ineffective nodules and reflect most likely an intense host-cell activity. The apparent proximity between some RER segments and peribacteroid envelopes leads us to speculate that RER may be implicated in the degenerative process of bacteroids, as already suggested by MacKenzie and Jordan (1974). Moreover, peroxisomes presented a very restricted development in uninfected cells of ineffective nodules of *Phaseolus vulgaris*. Peroxisomes are known to be the site of uricase activity, involved in the assimilation of fixed nitrogen (Van den Bosch et al. 1985; Newcomb et al. 1985; Webb and Newcomb 1987). Thus it is likely that the inability of the mutant bacteroids to fix nitrogen in substantial amounts is the cause of the restricted development of the peroxisomes.

A novel, surprising observation in mutant-infected cells was the occurrence of numerous spherical, laminated structures in plastids; these structures were often surrounded by organelles resembling elongated mitochondria. Although this association recalled that previously described by Werner and Mörschel (1978) between amyloplasts and mitochondria, the possibility that the multilayered structures could correspond to starch granules was disregarded in view of the cytochemical results obtained with the exoglucanase-gold complex. The intense and specific gold labeling observed over these structures indicated the presence of substantial amounts of cellulosic β-1,4-glucans. Since such polysaccharides were lacking in typical starch granules occurring in adjacent uninfected cells (see Fig. 14), it can be assumed that the laminated structures found only in plastids of infected cells of mutant-induced nodules are different from starch granules.

In infected cells of the WT, peripherally located plastids displayed also a specific labeling, thus indicating the presence of cellulosic β-1,4-glucans. However, these molecules were scattered throughout the matrices of these organelles instead of being organized to form laminated structures. These observations indicate that β-1,4-glucans are synthesized or accumulate in the plastid matrix of infected cells in both WT and mutant-induced

nodules of *Phaseolus vulgaris* cv. Goldie. By contrast, in uninfected cells, plastids are free of β-1,4-glucans and likely accumulate starch. In light of these results, one can consider that the enzyme activity of plastids in both WT- and mutant-infected cells is different from that of plastids in uninfected cells. This leads us to suggest that the plastid function in infected cells is modified as a consequence of the bacterial colonization.

At least two hypotheses may be proposed concerning the presence of β-1,4-glucans within the plastid matrix in WT-infected cells and the laminated structures in mutant-infected cells. First, it is possible that a cellulase produced by either the bacteroids or the host cell may have locally hydrolyzed the host cell-wall, thus releasing cellulose subunits (i.e. oligosaccharides composed of β-1,4-glucans) in the cytoplasm. By an unknown process, these β-1,4-glucans may have been transported in plastids, and gradually embedded by a cementing substance, thus giving rise to multilayered structures. Cellulase activity has been reported to occur in free-living form of *Rhizobium* (Martinez-Molina et al. 1979). The question of whether such a cellulase activity is still expressed in the bacteroid state remains to be clarified. Second, the possibility of a de-novo synthesis of β-1,4-glucans in the plastids of infected host cells cannot be ruled out. A time-course study of the appearance of the laminated structures should help in understanding their origin.

The presence of low amounts of β-1,4-glucans in bacteroids, as judged by the slight deposition of gold particles, indicates that these prokaryotes are potentially able to synthesize their own β-1,4-glucans or that they are able to take up such oligosaccharides. In an attempt to address this question, we have processed free-living bacteria of strain P_{121} and $P_{121}S_{21}$ for electron microscopy and tested them with the exoglucanase-gold complex to search for the presence of β-1,4-glucans oligosaccharides. The bacteria were grown on glucose, succinate or mannitol. Neither of the two bacteria types were labeled by the exoglucanase-gold complex, indicating the absence of constitutive or inducible β-1,4-glucans oligosaccharides (data not shown). Pea root nodules induced by a strain of *Rhizobium leguminosarum* bv. *viceae* were recently examined at the ultrastructural level (Chalifour and Benhamou 1989). Host cell-walls and infection-thread walls, known to contain cellulosic β-1,4-glucans, were densely labeled by the exoglucanase-gold complex. No other organelles or bacteroids were labeled. These results provide further support of the high specificity of the enzymatic probe used for cellulosic β-1,4-glucans detection.

This work was supported by grants from the Natural Sciences and Engineering Research Council of Canada to H. Antoun and N. Benhamou. The authors are grateful to Dr. E.H. Newcomb, Department of Botany, University of Wisconsin, Madison, USA, for helpful comments on the interpretation of the micrographs. We also wish to thank S. Noël and H. Bissonnette for excellent technical assistance, Mrs. M. Pelchat for typing this manuscript, and Dr. G.B. Ouellette, Centre Forestier des Laurentides, Agriculture Canada, Sainte-Foy, Que., Canada, for the use of his light microscope. Printing for this paper was supported by the Conseil des recherches et services agricoles du Québec.

References

Arwas, R., McKay, I.A., Rowney, F.R.P., Dilworth, M.J., Glenn, A.R. (1985) Properties of organic acid utilization mutants of *Rhizobium leguminosarum* strain 300. J. Gen. Microbiol. **131**, 2059–2066

Baird, L.M., Webster, B.D. (1982) Morphogenesis of effective and ineffective root nodules in *Phaseolus vulgaris*. L. Bot. Gaz. **143**, 41–51

Benhamou, N. (1989) Cytochemical localization of β-(1→4)-D-glucans in plant and fungal cells using an exoglucanase-gold complex. Electron Microsc. Rev. **2**, 123–138

Benhamou, N., Chamberland, H., Ouellette, G.B., Pauzé, F.J. (1987) Ultrastructural localization of β-(1→4)-D-glucans in two pathogenic fungi and in their host tissues by means of an exoglucanase-gold complex. Can. J. Microbiol. **33**, 405–417

Bergersen, F.J. (1957) The structure of ineffective nodules of legumes: an unusual type of ineffectiveness and an appraisal of present knowledge. Aust. J. Biol. Sci. **10**, 233–242

Berghem, L.E.R., Pettersson, L.G. (1973) The mechanism of enzymatic cellulose degradation. Purification of a cellulocytic enzyme from *Trichoderma viride* active on highly ordered cellulose. Eur. J. Biochem. **37**, 21–30

Berghem, L.E.R., Pettersson, L.G., Axiö-Fredricksson, U.-B. (1975) The mechanism of enzymatic cellulose degradation. Characterization and enzymatic properties of a β-1,4-glucan cellobiohydrolase from *Trichoderma viride*. Eur. J. Biochem. **53**, 55–62

Chalifour, F.-P., Benhamou, N. (1989) Indirect evidence for cellulase production by *Rhizobium* in pea root nodules during bacteroid differentiation: cytochemical aspects of cellulose breakdown in rhizobial droplets. Can. J. Microbiol. **35**, 821–829

Dazzo, F.B., Truchet, G.L. (1983) Interactions of lectins and their saccharide receptors in the *Rhizobium*-legume symbiosis. J. Membr. Biol. **73**, 1–16

Doherty, D., Leigh, J.A., Glazebrook, J., Walker, G.C. (1988) *Rhizobium meliloti* mutants that overproduce the *R. meliloti* acidic calcofluor-binding exopolysaccharide. J. Bacteriol. **170**, 4249–4256

Finan, T.M., Wood, J.M., Jordan, D.C. (1983) Symbiotic properties of C_4-dicarboxylic acid transport mutants of *Rhizobium leguminosarum*. J. Bacteriol. **154**, 1403–1413

Frens, G. (1973) Controlled nucleation for the regulation of the particle size in monodisperse gold solutions. Nature (London), Phys. Sci. **241**, 20–22

Huber, J.D., Parker, F., Odland, G.F. (1968) A basic fuchsin and alkalinized methylene blue rapid stain for epoxy-embedded tissue. Stain Technol. **43**, 83–87

Lafontaine, P.J., Lafrenière, C., Antoun, H. (1989a) Some properties of carbohydrate and C_4-dicarboxylic acid utilization negative mutants of *Rhizobium leguminosarum* biovar *phaseoli* strain P_{121}. Plant Soil **120**, 195–201

Lafontaine, P.J., Lafrenière, C., Chalifour, F.-P., Dion, P., Antoun, H. (1989b) Carbohydrate and organic acid composition of effective and ineffective root nodules of *Phaseolus vulgaris* Physiol. Plant. **76**, 507–513

Lafrenière, C., Lafontaine, P.J., Marion, C., Antoun, H. (1987) Oxidation of substrate in organic acids utilization negative mutants and the wild type *Rhizobium meliloti* strain S_{14}. Plant Soil **101**, 73–78

Lalande, R., Antoun, H., Paré, T., Joyal, P. (1986) Effets de l'inoculation avec des sourches du *Rhizobium leguminosarum* biovar *phaseoli* sur le rendement et la teneur en azote du haricot (*Phaseolus vulgaris*). Naturaliste Can. (Rev. Ecol. Syst.) **113**, 337–346

Leigh, J.A. Lee, C.C. (1988) Characterization of polysaccharides of *Rhizobium meliloti exo* mutants that form ineffective nodules. J. Bacteriol. **170**, 3327–3332

Leigh, J.A., Reed, J.W., Hanks, J.F., Hirsh, A.M., Walker, G.C. (1987) *Rhizobium meliloti* mutants that fail to succinylate their

calcofluor-binding exopolysaccharide are defective in nodule invasion. Cell **51**, 579–587

Long, S.R. Cooper, J. (1988) Overview of symbiosis. In: Proc. 4th Int. Symp. Mol. Gen. Plant Microbe Interact., Acapulo, Mexico, pp. 163–177, Palacios, R., Verma, D.P.S., eds. American Phytopathological Society, Press, St. Paul, Minn., USA

Long, S., Reed, J.W., Himawan, J., Walker, G.C. (1988) Genetic analysis of a cluster of genes required for synthesis of the calcofluor-binding exopolysaccharide of *Rhizobium meliloti*. J. Bacteriol. **170**, 4239–4248

Martinez-Molina, E., Morales, V.M., Hubbell, D.H. (1979) Hydrolytic enzyme production by *Rhizobium*. Appl. Environ. Microbiol. **38**, 1186–1188

MacKenzie, C.R., Jordan, D.C. (1974) Ultrastructure of root nodules formed by ineffective strains of *Rhizobium meliloti*. Can. J. Microbiol. **20**, 755–758

Newcomb, W., Syono, K., Torrey, J.G. (1977) Development of an ineffective pea root nodule: morphogenesis, fine structure, and cytokinin biosynthesis. Can. J. Bot. **55**, 1891–1907

Newcomb, E.H., Tandon, Sh.R., Kowal, R.R. (1985) Ultrastructural specialization for ureide production in uninfected cells of soybean root nodules. Protoplasma **125**, 1–12

Nogueira, N.D.L., Da Silva, D.M., Saito, S.M.T. (1979) Estudo ao microscopio eletrônico de nodulos em *Phaseolus vulgaris* L. causados por uma estripe inefetiva de *Rhizobium*. Turrialba **29**, 93–96

Pankhurst, C.E. (1974) Ineffective *Rhizobium trifolii* mutants examined by immune-diffusion, gel-electrophoresis and electron microscopy. J. Gen. Microbiol. **82**, 405–413

Ronson, C.W., Lyttleton, P., Robertson, J.G. (1981) C_4-dicarboxylate transport mutants of *Rhizobium trifolii* form ineffective nodules on *Trifolium repens*. Proc. Natl. Acad. Sci. USA **78**, 4284–4288

Selvaraj, G., Hooper, I., Shantharam, S., Iyer, V.N., Barran, L., Wheatcroft, R., Watson, R.J. (1987) Derivation and molecular characterization of symbiotically deficient mutants of *Rhizobium meliloti*. Can. J. Microbiol. **33**, 739–747

Van den Bosch, K.A., Noël, K.D., Kaneko, Y., Newcomb, E.H. (1985) Nodule initiation elicited by noninfective mutants of *Rhizobium phaseoli*. J. Bacteriol. **162**, 950–959

Watson, R.J., Chan, Y.-K., Wheatcroft, R., Yang, A.-F., Han, S. (1988) *Rhizobium meliloti* genes required for C_4-dicarboxylate transport and symbiotic nitrogen fixation are located on a megaplasmid. J. Bacteriol. **170**, 927–934

Webb, M.A., Newcomb, E.H. (1987) Cellular compartimentation of ureide biogenesis in root nodules of cowpea (*Vigna unguiculata* (L.) Walp.). Planta **172**, 162–175

Werner, D., Mörschel, E. (1978) Differentiation of nodules of *Glycine max*. Ultrastructural studies of plant cells and bacteroids. Planta **141**, 169–177

Werner, D., Mörschel, E., Kort, R., Mellor, R.B., Bassarab, S. (1984) Lysis of bacteroids in the vicinity of the host cell nucleus in an ineffective (fix⁻) root nodule of soybean (*Glycine max*). Planta **162**, 8–16

Received 10 July; accepted 6 October 1989